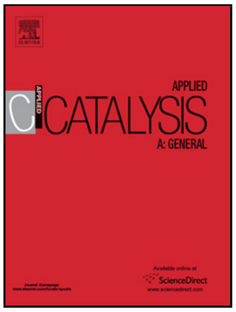

Title: Dehydration of D-xylose into furfural over bimetallic
salts of heteropolyacid in DMSO/H_2O mixture

Authors: Xiaoqian Guo, Feng Guo, Yishan Li, Zhangqin
Zheng, Zhexu Xing, Zihan Zhu, Ting Liu, Xin Zhang, Ying Jin

PII: S0926-860X(18)30146-7
DOI: https://doi.org/10.1016/j.apcata.2018.03.027
Reference: APCATA 16601

To appear in: *Applied Catalysis A: General*

Received date: 13-12-2017
Revised date: 7-3-2018
Accepted date: 26-3-2018

Please cite this article as: Guo X, Guo F, Li Y, Zheng Z, Xing Z, Zhu Z, Liu T, Zhang X, Jin Y, Dehydration of D-xylose into furfural over bimetallic salts of heteropolyacid in DMSO/H_2O mixture, *Applied Catalysis A, General* (2010), https://doi.org/10.1016/j.apcata.2018.03.027

Dehydration of D-xylose into furfural over bimetallic salts of heteropolyacid in DMSO/H_2O mixture

Xiaoqian Guo[1], Feng Guo[1]*, Yishan Li[2], Zhangqin Zheng[1], Zhexu Xing[1], Zihan Zhu[1], Ting Liu[1], Xin Zhang[2], Ying Jin[1]

[1]School of Food and Environment, Dalian University of Technology, Panjin Campus, 2 Dagong Road, Liaodong Bay New District, Panjin 124221, China

[2]School of Petroleum and Chemical Engineering, Dalian University of Technology, Panjin Campus, 2 Dagong Road, Liaodong Bay New District, Panjin 124221, China

Revised for *Applied Catalysis A: General*

(Jan. 2018)

* **Corresponding author:**

Tel.: +86-427-2631892.

E-mail Address: 0411guofeng@dlut.edu.cn (F. Guo);

Graphical abstract

Graphical abstract

Mesoporous bi-metallic salts of heteropoly acid was synthesized for the transformation of xylose into furfural in a DMSO-H_2O system. The introduction of Sn^{4+} into the structure of $Cs_{0.5}PW$ did not change the Keggin structure. Sn^{4+} occupied the surface available space of Cs^+, which helps improve catalytic performance toward xylose dehydration. Supported $Sn_{0.625}Cs_{0.5}PW/CH$ displayed similar catalytic activities with $Sn_{0.625}Cs_{0.5}PW$ and good stability after six cycles of recycling.

Research highlights

- ►A series of bi-metallic salts of heteropoly acid was synthesized for the conversion of xylose to furfural.
- ► Introduction of Sn^{4+} and Cs^+ did not change the Keggin-type structure of original heteropoly acid.
- ►Sn^{4+} occupied the surface available space of Cs^+, which helps improve the catalytic activity.
- ►The addition of DMSO can effectively improve the furfural selectivity.
- ► $Sn_{0.625}Cs_{0.5}PW/CH$ displayed similar catalytic activities with $Sn_{0.625}Cs_{0.5}PW$ and good stability after six cycles of recycling.

Abstract

Dehydration of D-xylose to yield furfural was carried out using bimetallic salts of a heteropolyacid as the catalyst at 160 – 220 °C in the DMSO/H_2O mixtures. The effect of Sn/Cs molar ratio of the bimetallic salts of 12-tungstophosphoric acid (PW) obtained by ultrasound-assisted coprecipitation on dehydration of D-xylose was investigated. The resultant catalysts were characterized by X-ray diffraction, N_2 adsorption, field emission scanning electron microscopy and energy dispersive X-ray (EDX). It was found that the Sn-Cs codoped PW catalysts retained the Keggin crystal structure of PW. $Sn_{0.625}Cs_{0.5}PW$ was the most active catalyst in the dehydration of D-xylose into furfural. The maximum D-xylose conversion (close to 100 wt %) and furfural yield (63 wt %) were achieved at 200 °C for 3 h in DMSO/H_2O mixtures. It was found that 16.7 wt % $Sn_{0.625}Cs_{0.5}PW$ on a chitosan-derived support displayed similar catalytic activity to that of $Sn_{0.625}Cs_{0.5}PW$ and good stability after recycling six times.

Keywords: D-xylose; furfural; dehydration; heteropolyacid salts; bimetallic salts

1. Introduction

The decrease of global fossil resources has become a driving force for the use of biomass as a resource. Development of renewable energy and chemicals from biomass lower the reliance on oil resources and can provide new products [1]. Rated as one of the top ten bio-based chemicals by the US Department of Energy, furfural could be used to sustainably produce C_4 and C_5 chemicals [2]. D-Xylose and pentosans are promising non-toxic renewable feedstock for furfural production through control of the dehydration conditions.

Researchers have conducted much work to improve the conversion efficiency of D-xylose to furfural through dehydration. However, the industrial production of furfural lacks competitive edge because the current technologies are inefficient with low yield of furfural [3]. Dehydration of D-xylose or hemicelluloses by traditional catalysts, such as mineral acid, heteropolyacid and metal salts, requiring a high temperature (~ 250 ℃) and long reaction time (24 h) [4]. In addition, these catalysts have many shortcomings, including equipment corrosion, high pollution and high energy consumption [5]. It has been suggested that development of dehydration technology and synthesizing heterogeneous catalyst should be effective methods to overcome these problems.

Heterogeneous catalysts receive considerable attention because of their easy recycling through simple filtration and ready operation as fixed beds [5]. The use of ionic liquids and high-pressure CO_2 for biomass conversion result in effective production of furfural without formation of humins [6-9]. These processes show good development prospects, because it integrates the processes of dissolution, fractionation, hydrolysis and conversion in one pot. Solvent recycling and decreased energy demand should make this approach technologically and economically viable. It is speculated that the combination of a heterogeneous catalyst with a suitable solvent will result in effective conversion of D-xylose to furfural.

Many different heterogeneous catalysts, such as Nafion [10], zeolite [11], Amberlyst-15 [12], SO_3H-MCM-41 [13], and as well as resorcinol-formaldehyde resin carbon [14], have been explored. However, most heterogeneous catalysts display deficiencies, such as low furfural yield (~ 30%), poor thermal stability, and high price [12, 14, 15]. Heteropolyacid salts exhibit promising furfural production performances. Heteropolyacid salts inherit most of the functions and characteristics of a heteropolyacid, e.g., non-explosive, strong acidity, and strong oxidizing capability [16]. However, apart from cesium salts (Cs) of heteropolyacid (denoted as $Cs_xH_{3-x}PW_{12}O_{40}$), heteropolyacid salts have many shortcomings, such as low surface area and high solubility in polar solvents [17]. It has been reported that the acidity of heteropolyacid Cs has the order of $H_3PW_{12}O_{40} > Cs_2HPW_{12}O_{40} > Cs_{2.5}H_{0.5}PW_{12}O_{40}$ [18]. However, the acidic Cs salt $Cs_3PW_{12}O_{40}$ has a much higher surface area (~200 m^2/g) than that of the initial heteropolyacid $H_3PW_{12}O_{40}$ (~5 m^2/g) [19]. Meanwhile, an increase in the content of acidic sites on the surface induced by Cs^+/H^+ exchange changes the catalytic capability of $Cs_xH_{3-x}PW_{12}O_{40}$. The initial activities of these catalysts for D-xylose dehydration displayed the order of $H_3PW_{12}O_{40} < Cs_{2.0}H_1PW_{12}O_{40} < Cs_{2.5}H_{0.5}PW_{12}O_{40}$ [20]. Moreover, the increasing Cs^+ substitution of $Cs_xH_{3-x}PW_{12}O_{40}$ could increase the hydrophobicity of the heteropoly compounds. This makes $Cs_xH_{3-x}PW_{12}O_{40}$ exhibit high stability in aqueous media.

Heteropolyacid cesium salts usually forms colloidal suspensions in polar media (i.e., H_2O) making it difficult to reuse the solid catalyst [21]. One solution to this problem would be to support the heteropolyacid cesium salts on a carrier such as SiO_2, ZrO_2, TiO_2, MCM-41, or SBA-15 [22, 23]. These catalyst supports have been used extensively for various organic reactions such as hydrogenation, dehydration, hydrolysis, alkylation, acylation and esterification reactions [24-28]. On the other hand, these materials demonstrate lower activity and selectivity than those of for $Cs_xH_{3-x}PW_{12}O_{40}$. It has been reported that heteropolyacid catalysts with Lewis acidity exhibit high catalytic efficiency and mild specificity [29]. Therefore, introducing a Lewis acid into $Cs_xH_{3-x}PW_{12}O_{40}$ would change its catalytic properties and selectivity considering that $Cs_xH_{3-x}PW_{12}O_{40}$ already has high surface area and Brønsted acidity.

In this study, some of water-soluble heteropolyacid salts are first prepared. The catalyst cations are substituted by Cs^+ to form heterogeneous bi-metallic salts of the heteropolyacid. The Keggin crystal structures of the catalysts are investigated. Then, the dehydration of D-xylose to form furfural catalyzed by the bimetallic heteropolyacid salts and the influence of reaction parameters on D-xylose dehydration are studied. Catalyst stability is also studied by recycling experiments.

2. Experiment

2.1 Materials

12-tungstophosphoric acid ($H_3PW_{12}O_{40}\cdot xH_2O$, 99+% purity) and cesium chloride (99+% purity) used for the catalyst preparation were purchased from J&K® Scientific Ltd. (Beijing, China). Stannic chloride pentahydrate (99% purity), Ferric chloride hexahydrate (99% purity), potassium chloride (99.5% purity), nickel chloride hexahydrate (98% purity), cerium nitrate hexahydrate (99% purity), ammonium sulfate (99% purity), rubidium chloride (99% purity), and dimethyl sulfoxide (99% purity) were bought from Damao Chemical Reagent Factory (Tianjin, China) and used for catalyst preparation without further purification. D-xylose in conversion experiments was obtained from Aladdin Reagent Co., Ltd. (Shanghai, China). Standard furfural (99% purity) and D-xylose (99% purity) were purchased from Sigma-Aldrich (Shanghai, China).

2.2 Preparation and characterization of catalysts

Catalysts were prepared in a 200-mL Teflon hydrothermal vessel. In the presence of ultrasonic irradiation, 20 mL of 1.8 mM metal chloride (e.g. $SnCl_4$, $FeCl_2$, $CuCl_2$, $NiCl_2$, $(NH_4)_2SO_4$, or KCl) aqueous solution was added dropwise to 100 mL of a 1 mM aqueous solution of $H_3PW_{12}O_{40}$. Subsequently, 20 mL of 5 mM CsCl (or RbCl) aqueous solution was added dropwise, which gave a milky precipitate. The reaction Teflon vessel was then immersed in a thermostat-controlled oil-bath controlled at 200 °C with vigorous magnetic stirring. After a certain reaction time, the mixture was cooled to room temperature, centrifuged, and then washed with deionized water until the rinsing water reached a pH of 6–7. The resulting sample was dried by lyophilization and then used a catalyst. In addition, a chitosan–derived carbon material (CH) supported catalyst was prepared via a similar process except that a certain amount of chitosan was dissolved in the aqueous solution of $H_3PW_{12}O_{40}$ solution in advance. The catalyst loading occurred in parallel with the preparation of the catalyst carrier. The catalyst loading was 30 wt %. All experiments were repeated three times, and the reported values are the averages of the three replicates.

The crystal structure of the catalysts was analyzed using X-ray diffraction (XRD; XRD-7000s, Shimadzu, Japan), measured with CuKα (λ = 0.154 nm) radiation at 40 kV and 20 mA by scanning at a rate of 5°/min in the 2θ range of 5 – 100°. Scans were collected by an X-ray diffractometer control and data acquisition system (MDI, US). The microstructure of the catalysts was characterized using a Nova NanoSEM 450 (FEI) field-emission scanning electron microscope (FE-SEM) equipped with an energy dispersive X-ray (EDX) spectrometer operating at an acceleration voltage of 20 kV and working distance of 5 mm. The catalysts were dried and sprayed with gold before FE-SEM analysis. Specific surface areas were determined by N_2 adsorption at 77 K with the Brunauer-Emmett-Teller (BET) method using an Autosorb-iQ-C chemisorption analyzer (Quantachrome Instruments). Surface functional groups of solid catalysts were characterized by Fourier transform infrared (FT-IR) spectroscopy (ThermoFisher Scientific, USA) using an ATR cell with a scanning range from 700 to 1500 cm^{-1}.

2.3 Experimental procedure

A 20-mL autoclave equipped with a Teflon-lined hydrothermal vessel and microwave reactor (MDS-6G, Shanghai) equipped with eight 50-mL Teflon vessels were used for the dehydration experiments. The Teflon-lined hydrothermal vessel was charged with D-xylose, catalyst, and reaction medium. The vessel was subsequently sealed in the reactor and placed in a circulating constant-temperature oil bath (or microwave reactor). In a typical procedure, 0.1 g D-xylose, 0.08 g $Sn_{0.625}Cs_{0.5}PW$ and 20 ml solvent were put in the Teflon vessel and reacted at the set temperature (160–200 °C) with magnetic stirring at 400 rpm.

2.4 Analytical methods

D-xylose was analyzed by high-performance liquid chromatography (HPLC; Ultimate 3000, US) fitted with an Aminex HPX-87H column (Bio-Rad, Richmond, CA) and refractive index (RI) detector. Furfural was determined using the same column, but was measured with an ultraviolet (UV) detector at 280 nm. The column temperature was set at 50 °C. The mobile phase was 5 mM of H_2SO_4 at a flow rate of 0.6 ml/min.

D-xylose conversion rate (X, mol%) and furfural yield (Y, mol%) were calculated as follows:

$$X=\left(1-\frac{\text{mol concentration of D-xylose in products}}{\text{mol concentration of initial D-xylose}}\right)\times 100\% \qquad (1)$$

$$Y=\left(\frac{\text{mol concentration of furfural}}{\text{mol concentration of initial D-xylose}}\right)\times 100\% \qquad (2)$$

3. Result and Discussion

3.1 FE-SEM analysis

The microtopography of the bimetallic salt-exchanged PW catalysts were observed by FE-SEM. The morphology of $Cs_{0.5}H_{2.5}$PW was heterogeneous spherical particles, as shown in Fig. 1(a). Spherical particles of submicron size with a particle size distribution between 100 and 500 nm were obtained for $Cs_{2.5}H_{0.5}$ PW (Fig. 1b). The surface of these particles still remained rough. These particles were composed of aggregates of small spherical particles obtained via re-crystallization during hydrothermal preparation.

The introduction of Sn^{4+} into the mono-cationic salts caused the formation of agglomerates with an irregular particle size of less than 250 nm (Fig. 1c and d). The average particle size and distribution range of $Sn_{0.625}Cs_{0.5}$PW were similar to those of $Sn_{0.5}$CsPW. In addition, both $Sn_{0.5}$CsPW and $Sn_{0.625}Cs_{0.5}$PW have rough surfaces. Such surface structure permits access of reactants to the active sites, which is required to realize the catalytic activity of these heteropolyacids. Sn_xRb_{3-4x}PW was obtained via Sn^{4+} substitution for Rb^+ and H^+ in Rb_xH_{3-x}PW. When Cs^+ was substituted by Rb^+, the surface of $Sn_{0.55}Rb_{0.8}$PW became smoother than that of $Sn_{0.625}Cs_{0.5}$PW (Fig. 1e). In this study, a chitosan-derived carbon material (denoted as CH) was used as a catalyst carrier to anchor catalytic species. Fig. 1f shows that CH has layered-stacking arrangements because of the synergistic effects of the hydrothermal process and heteropolyacid salts. The structures of $Cs_{2.5}H_{0.5}$PW and $Sn_{0.625}Cs_{0.5}$PW were maintained after loading on the surface of the CH carrier (Fig. 1g and h). It can be seen that submicron catalyst particles were uniformly dispersed on the surface of CH. CH has abundant surface functional groups, such as C-OH, COOH and C=O [30, 31]. Such groups are conductive to achieve rapid adsorption of substrates during the contact phase.

3.2 EDX study

Both solid bi-metallic and Cs of heteropolyacid can convert D-xylose into furfural effectively. Besides number of surface active sites, catalytic species usually play a decisive role in reactions catalyzed by solid catalysts. EDX analysis of the synthesized heteropolyacid salts was conducted to assess their elemental distributions. The EDX spectra revealed the presence of P, W, O, Sn, Cs (or Rb) elements in the heteropolyacid salts (Fig. S1).

According to the EDX area analysis of $Sn_{0.625}Cs_{0.5}PW$ (Fig. S1b), the determined Sn/Cs atomic ratio was 1.68, which is higher than that of the theoretical value (1.25). This indicates that excess Sn^{4+} is distributed on the crystal surface of the heteropolyacid salt. $Sn_{0.625}Cs_{0.5}PW$ displayed the highest catalytic activity in the dehydration of D-xylose of the investigated catalysts. It is speculated that Sn^{4+} occupied the available surface site of Cs^+ and consequently achieved excellent dehydration activity. Furthermore, the substitution of H^+ by Rb^+ was more stable than that of substitution by Cs^+, as confirmed by the EDX spectrum in Fig. S1c. It can be seen that Rb^+ (EDX area of 34%) was preferentially distributed on the surface of the solid catalyst compared with the case for Cs^+ (EDX area of 13%). However, $Sn_{0.55}Rb_{0.8}PW$ showed lower dehydration activity than that of $Sn_{0.65}Rb_{0.5}PW$. This further proves that a high distribution of Sn^{4+} helps to improve catalytic performance in D-xylose dehydration. After $Sn_{0.625}Cs_{0.5}PW$ was supported on CH, the Sn/Cs atomic ratio decreased from 1.69 to 1.375. The presence of carbon in the EDX images reveals the interference of C with Sn distribution.

3.3 XRD study

XRD analysis was used to evaluate the crystalline structure of the unsupported and CH-supported bimetallic heteropolyacid salts, as shown in Fig. 2. All catalysts possessed the same crystalline structure because all peaks existed at similar position. The Keggin structure of PW compounds was confirmed by the presence of diffraction peaks at $2\theta$of 8°–10°, 17°–20°, 26°–30° and 33°–35°. The XRD patterns of $Sn_{0.625}Cs_{0.5}PW$ showed diffraction peaks at $2\theta=10.3°$, 18.0°, 21.0°, 23.3° and 30.2°, which are consistent with cubic system [32]. This was also confirmed by FT-IR spectroscopy (Fig. S2a). The FT-IR spectra displayed the characteristic features of a Keggin-type structure of four bands at 1077, 982, 885 and 778 cm^{-1}, which corresponded to P-O, W = O, W – O – W, and W – O – W asymmetric vibrations [33], respectively.

No diffraction peak confirming the existence of Sn-O or Sn-OH was observed, indicating that Sn^{4+} substitution did not change the structure of the Keggin anion. The most intense peaks were observed at around 27°, indicating that the Cs-substituted PW catalysts had crystalline structures. Moreover, the diffraction peak at around 27° shifted to higher diffraction angle as the Cs^+ content increased (Fig. 2a-c). This peak shift behavior was caused by the decrease of lattice constant and loss of water from the crystal [34]. The diffraction peaks for $Sn_{0.625}Cs_{0.5}PW/CH$ suggested that the Keggin structure remained after heteropolyacid immobilization. FT-IR data also indicated that the

Keggin structure was retained when loading $Sn_{0.625}Cs_{0.5}PW$ on CH (Fig. S2b). After immobilization, the three characteristic bands at 982, 885 and 778 cm^{-1} shifted to 986, 889 and 807 cm^{-1}, respectively. This may be partially caused by the formation of ion pair between $Sn_{0.625}Cs_{0.5}PW$ and the amine groups in CH [35].

3.4 N_2 adsorption

Figure 3 shows the N_2 adsorption–desorption isotherm and Barrett–Joyner–Halenda pore size distribution curve of $Sn_{0.625}Cs_{0.5}PW$. $Sn_{0.625}Cs_{0.5}PW$ presents typical Langmuir type–II adsorption–desorption isothermal curves, which is a consistent with clustered particles. This conclusion agrees with the morphology of $Sn_{0.625}Cs_{0.5}PW$ observed by FE-SEM (Fig. 1(d)). It has been reported that the specific surface area of PW and Cs^+–doped PW are 5 and 156 m^2/g, respectively [36]. In this study, as seen in Table 2, the surface area of $Sn_{0.625}Cs_{0.5}PW$ calculated from the linear part of its BET plot is 140 m^2/g. Obviously, Sn-Cs substitution of PW can increase its surface area. The determined pore volume and diameter of $Sn_{0.625}Cs_{0.5}PW$ are 0.32 cm^3/g and 11 nm, respectively. The mesoporous structure of $Sn_{0.625}Cs_{0.5}PW$ is conducive to the ion-exchange between Sn^{4+} and Cs^+. After $Sn_{0.625}Cs_{0.5}PW$ was supported on the surface of CH, the BET surface area increased to 219 m^2/g and the pore diameter increased to 9.6 nm. These results may be favorable because mesoporous catalysts usually exhibit much higher catalytic activities, as a result of facile substrate molecular diffusion to the catalytic sites in the internal pores.

3.5 Catalyst testing

3.5.1 Catalysts screening

All of the catalysts were prepared under the same conditions: hydrothermal treatment at 200 °C for 2 h in a Teflon-lined vessel. Eight solid catalysts were synthesized and all exhibited D-xylose conversion rates of nearly 100%. For comparison, H_2SO_4, HCl and CH_3COOH were used to catalyze D-xylose dehydration under the same conditions, as shown in Fig. 4. The catalytic activity of the tested catalysts tested decreased with the order of $H_2SO_4 > HCl > CH_3COOH > Sn_{0.625}Cs_{0.5}PW > H_2RbPW > H_{0.5}Cs_{2.5}PW > HKCsPW > H_{0.5}Fe_{0.5}PW > HNi_{0.5}CsPW > H_{0.5}Ce_{0.5}CsPW$. Thus, $Sn_{0.625}Cs_{0.5}PW$ showed the highest activity among all the metallic ion exchanged PW catalysts, with a furfural yield of 44%. This is because Sn^{4+} occupied the available surface sites of Cs^+ on the spherical particle surface of the Keggin crystal. Addition of transition metals could influence the catalytic activity of PW when they are incorporated in the primary structure of the Keggin unit [37].

H_2RbPW has a strong preference towards surface cation distribution but exhibited similar catalytic activity (34.5%) to that of $H_{0.5}Cs_{2.5}PW$. This supports the notion that the cation distribution of Rb^+ and Cs^+ has little effect on structure and acidity of PW. Other M-Cs^+ (M = Fe^{2+}, Ni^{2+}, Al^{3+}, NH_4^+ or Ce^{4+}) substituted HPW catalysts, displayed much lower the furfural yields of less than 11%.

A series of $Sn_xCs_{3-4x}PW$ (x = 0.25, 0.50, 0.55 and 0.625) catalysts were further synthesized to study the effect of surface distribution of Sn^{4+} and Cs^+ on furfural yield. Table 1 shows that furfural yield indeed increased slightly with the content of Sn^{4+} on the surface of $Sn_xCs_{3-4x}PW$. The optimal attribution ratio of Sn^{4+} was 0.625, in which case a furfural yield of 44.4% was achieved in 3.5 h at 200 °C with 99% D-xylose conversion. A higher theoretical value of Sn^{4+} during $Sn_xCs_{3-4x}PW$ preparation gave no further significant increase in surface Sn^{4+} content; instead, catalytic activity decreased. Therefore, $Sn_{0.625}Cs_{0.5}PW$ was selected for the following dehydration reactions.

3.5.2 Dehydration of D-xylose

The effect of variables on D-xylose dehydration with $Sn_{0.625}Cs_{0.5}PW$ in different media was studied (Fig. 5–7). Compared with water, DMSO/H_2O mixtures lowered the required reaction temperature to 180 °C (*vs*. 200 °C) and time to 3 h (*vs*. 3.5 h) while increasing the furfural yield from 44% to 63% (Fig. 5). This may be partially because DMSO effectively inhibited the progressive transformation of the target furfural [30, 38]. DMSO has advantage of a high boiling point, making it a useful solvent in industrial applications.

Increasing in the concentration of D-xylose from 5 to 10 g/L led to a remarkable decrease in the furfural yield from 63% to 15%. It is known that the water negatively affects furfural formation because water accelerates furfural degradation reactions [39]. Therefore, using water as the reaction medium led to the low selectivity. The leading published researches on heterogeneous solid acid catalyzed dehydration in aqueous media have wide initial D-xylose concentration ranges from 1 wt% to 15 wt% [40, 41]. In this study, higher D-xylose concentrations caused a considerable decrease of furfural selectivity. This issue could be solved by using ILs or supercritical CO_2 as co-solvent [6-9], but there are many theoretical and technical problems remain open, such as high cost of ILs and product separation difficulty. In this study, lowering the reaction temperature and extending the reaction time is one of the feasible ways. However, higher D-xylose concentration will result in an increase yield of humins by-product [42], and definitely influence on the stability and activity of $Sn_{0.625}Cs_{0.5}PW$. 5 g/L was selected as an acceptable D-xylose concentration in subsequent reactions.

It has been reported that the condensation of furfural and D-xylose causes a decrease of furfural selectivity [30]. Furan and formic acid are the main by-products in D-xylose dehydration at high temperature. Therefore, the addition of DMSO can effectively decrease the formation of by-products. It should be noted that the addition of water is desirable for increasing the solubility of D-xylose [43]. In addition, water can act as an amphoteric substance capable of donating and accepting protons during the dehydration process [44]. An appropriate amount of water is necessary to obtain a high furfural yield. Moreover, the addition of organic solvent was beneficial to inhibit furfural yield-loss reactions that lead to the polymerization of furfural and D-xylose.

To understand the effects of solvent on furfural selectivity, the conversion of D-xylose was investigated in different solvents (Fig. 6). It was found that the furfural selectivity in solvent-H_2O mixtures decreased in the order of DMSO > butanol > ethanol > isopropanol > acetone. The solvents used covered a wide range of polarity. Ketones (i.e., acetone) are very reactive and can react with both D-xylose and furfural [45]; therefore, acetone gave the lowest yield of furfural (38%). The furfural yield was greatly enhanced in alcohols/H_2O mixtures. To a certain extent, alcohols can prevent the polymerization of furfural by inhibiting aldol condensation [44]. DMSO achieved the transformation of D-xylose into furfural with the highest selectivity of 63%. DMSO has the lowest polarity and highest boiling point (189 °C) of the investigated solvent, and these properties would be favorable for the dissolution of furfural and separation of products, respectively.

The reaction temperature also had a considerable effect on the degree of D-xylose dehydration. It is generally known that furfural molecules in the vapor phase cannot undergo loss reactions [45]. The influence of temperature on the dehydration reaction was studied in the range of 160–220 °C (Fig. 7). At 160 °C for 3 h, a 26.5% yield of furfural was achieved. Furfural yield increased obviously as temperature was increased from 160 °C to 200 °C, at which a maximum of 64% was achieved. Further increase of temperature caused a decrease of furfural yield to 42%. The loss of furfural was attributed to cross- and self-polymerization [46]. The resultant solid products are called insoluble humins. Correspondingly, the color of the product varied from light yellow to brown, showing the reaction of D-xylose and furfural to produce humins and other decomposition products. In this study, an insoluble humins yield of 1.21 g/L was obtained at 220 °C. The increase in soluble humins yield was higher than the decrease in furfural yield (1.1 g/L). The insoluble humins were deposited on the outer surface of the solid catalyst, leading to a decrease in catalyst acidity [42]. Therefore, the optimum reaction temperature of 200 ^{o}C was used in subsequent experiments.

In a review, different heterogeneous acid catalysts, especially mesoporous acid-catalysts, were summarized to provide a general overview of heterogeneous catalysts studies [40]. Compared with other heterogeneous acid catalysts with furfural yields of 10%–65% in organic solvent/H_2O mixtures in the above review [40], $Sn_{0.625}Cs_{0.5}PW$ exhibited relatively high catalytic efficiency. Taking into account the reaction media, the reaction in DMSO/H_2O mixtures was less active than that in ionic liquids. However, it should be noted that the DMSO/H_2O system has a cost advantage over that of ionic liquids.

3.6 Supported $Sn_{0.625}Cs_{0.5}PW$

A carrier to support $Sn_{0.625}Cs_{0.5}PW$ was prepared by incomplete carbonization of chitosan via a hydrothermal process at 220 °C for 8 h. The supported $Sn_{0.625}Cs_{0.5}PW$ prepared by hydrothermal deposition process was studied. The effects of $Sn_{0.625}Cs_{0.5}PW$ addition on carbonization of chitosan were determined by changing the $Sn_{0.625}Cs_{0.5}PW$ loading, as shown in Fig. 8. The maximum furfural yield of 62% was achieved using 16.7 wt % $Sn_{0.625}Cs_{0.5}PW$/CH. Increasing the $Sn_{0.625}Cs_{0.5}PW$ loading from 16.7 wt % to 50 wt % caused the furfural yield to drop from 62% to 28%. These results indicated that 16.7 wt % $Sn_{0.625}Cs_{0.5}PW$/CH prossessed similar catalytic activity to that of $Sn_{0.625}Cs_{0.5}PW$. Thus, 16.7 wt % $Sn_{0.625}Cs_{0.5}PW$/CH is active as a heterogeneous systems as well as being recoverable and reusable.

3.7 Catalyst stability

Recycling of 16.7 wt % $Sn_{0.625}Cs_{0.5}PW$/CH was conducted in a DMSO/H_2O mixture at 200 °C, for 3 h with D-xylose/16.7 wt % $Sn_{0.625}Cs_{0.5}PW$/CH weight ratio of 1.25. After one batch reaction, the solid $Sn_{0.625}Cs_{0.5}PW$/CH was separated from the mixture by centrifugation, washed with deionized water, dried then used in the next dehydration process. Both D-xylose conversation rate and furfural yield slightly decreased with an increasing number of recycling runs (Fig. 9). A furfural yield of 63% was achieved for the first use of 16.7 wt $Sn_{0.625}Cs_{0.5}PW$/CH, which decreased to 57% after the catalyst was recycled four times. After the 16.7 wt % $Sn_{0.625}Cs_{0.5}PW$/CH was reused in six runs, the furfural yield was still 54.2%. The EDX pattern of 16.7 wt % $Sn_{0.625}Cs_{0.5}PW$/CH after five cycling experiments is shown in Fig. S3. The atomic ratios of C and O increased considerably, which can be explained by the adsorption and deposition of formed solid humins on the surface of $Sn_{0.625}Cs_{0.5}PW$/CH. As a result, the atomic ratios of Sn^{4+} and Cs^{+} decreased accordingly. The cycling experiments showed that the catalytic activity of the supported solid catalysts was stable. The good stability of the catalyst is probably caused by its large surface area and pore volume, uniform distribution of $Sn_{0.625}Cs_{0.5}PW$ on CH, and resistance to leaching. The slight activity decrease was possibly caused by the adsorption and deposition of humins.

This methodology was also suitable for the dehydration of xylose-rich liquors from biomass pre-treatment. Renewable bio-mass, which contains rich cellulose and hemicellulose, are potential starting materials for the manufacture of furans. The furfural yields obtained from xylan were usually lower than those from D-xylose. The transformation of D-xylose to furfural depends on the real concentration of D-xylose released during the biomass pre-treatment. One-pot process combining excellent solubility (i.e., ionic liquids) and microwave-assisted heating will be attempted to improve the furfural yield.

Conclusion

A series of bi-metallic salts of heteropoly acid was synthesized for the conversion of D-xylose to furfural in a DMSO-H_2O system. The introduction of Sn^{4+} into the structure of $Cs_{0.5}PW$ did not change its Keggin structure, but caused the particle size to increase to 250 nm. Sn^{4+} occupied the available surface sites of Cs^+, which helped improve its catalytic performance in D-xylose dehydration. The addition of DMSO effectively improved the furfural selectivity of the system. The highest furfural yield of 63% with a conversion efficiency of 98% and furfural selectivity of 84.3% was obtained after 3 h at 200 °C in a DMSO/H_2O mixture with a 1:1 volume ratio. The supported 16.7 wt % $Sn_{0.625}Cs_{0.5}PW$/CH catalyst displayed similar catalytic activity to that of unsupported $Sn_{0.625}Cs_{0.5}PW$ and good stability after recycling six times.

Acknowledgement

The authors wish to acknowledge the financial support from Dalian University of Technology (DUT15RC(3)114) and China National Natural Science Foundation (No: 31270620). We thank Natasha Lundin, PhD, from Liwen Bianji, Edanz Editing China, for editing the English text of a draft of this manuscript.

Reference

[1] O. Ellabban, H. Abu-Rub, F. Blaabjerg, Renew. Sust. Energ. Rev. 39 (2014) 748-764.

[2] J.J. Bozell, G.R. Petersen, Green Chem. 12 (2010) 539-554.

[3] X. Li, P. Jia, T. Wang, ACS Catal. 6 (2016) 7621-7640.

[4] I. Agirrezabal-Telleria, I. Gandarias, P.L.Arias, Catal. Today 234 (2014) 42-58.

[5] J.P. Lange, E. van der Heide, J. van Buijtenen, R. Price, ChemSusChem 5 (2012) 150-166.

[6] S. Peleteiro, G. Garrote, V. Santos, J.C. Parajó, Afinidad, 71 (2014) 202-206.

[7] S. Peleteiro, A.M. da Costa Lopes, G. Garrote, J.C. Parajó, R. Bogel-Łukasik, Ind. Eng. Chem. Res. 54 (2015) 8368-8373.

[8] Z. Fang, R.L.J. Smith, X. Qi (Eds.), Production of Platform Chemicals from Renewable Resources, Springer, 2017, pp. 45-80.

[9] A.M. da Costa Lopes, R. Bogel‐Łukasik, Green Chem. 8 (2016) 2331-2334.

[10] E. Lam, E. Majid, A.C.W. Leung, J.H. Chong, K.A. Mahmoud, J.H.T. Luong, ChemSusChem 4 (2011) 535-541.

[11] S.M. Bruce, Z. Zong, A. Chatzidimitriou, L.E. Avci, J.Q. Bond, M.A. Carreon, S.G. J. Wettstein, Mol. Catal. A-Chem 422 (2016) 18-22.

[12] W. Jeon, C. Ban, J.E. Kim, H.C. Woo, Kim D.H. J., Mol. Catal. A-Chem 423 (2016) 264-269.

[13] S. Kaiprommarat, S. Kongparakul, P. Reubroycharoen, G. Guan, C. Samart, Fuel 174 (2016) 189-196.

[14] Y. Zhu, W. Li, Y. Lu, T. Zhang, H. Jameel, H. Chang, L. Ma. RSC Adv. 7(2017) 29916-29924.

[15] M.J. Climent, A. Corma, S. Iborra, Chem. Rev. 111 (2011) 1072-1133.

[16] M.M. Heravi, Z. Faghihi, J. Iran. Chem. Soc. 11 (2014) 209-224.

[17] G. Raveendra, M. Srinivas, N. Pasha, A.V.P. Rao, P. S.S. Prasad, N. Lingaiah, React. Kinet. Mech. Cat. 115 (2015) 663-678.

[18] G. Marcì, E.I. García-López, L. Palmisano, Eur. J. Inorg. Chem. 2014, 21-35.

[19] T. Okuhara, Chem. Rev. 102 (2002) 3641-3666.

[20] A.S. Dias, S. Lima, M. Pillinger, A.A. Valente, Carbohydr. Res. 341 (2006) 2946-2953.

[21] P.M. Rao, M.V. Landau, A. Wolfson, A.M. Shapira-Tchelet, M. Herskowitz, Microporous Mesoporous Mat. 80 (2005) 43-55.

[22] A.M. Alsalme, P.V. Wiper, Y.Z. Khimyak, E.F. Kozhevnikova, I.V. Kozhevnikov, J. Catal. 276

(2010) 181-189.

[23] K.M. Parida, S. Rana, S. Mallick, D. Rath, J. Colloid Interface Sci. 350 (2010) 132-139.

[24] J. Geboers, S.V. Vyver, K. Carpentier, P. Jacobs, B. Sels, Green Chem. 13 (2011) 2167-2174.

[25] W. Alharbi, E. Brown, E.F. Kozhevnikova, I.V. Kozhevnikov, J. Catal. 319 (2014) 174-181.

[26] S. Tsubaki, K. Oono, T. Ueda, A. Onda, K. Yanagisawa, T. Mitani, J. Azuma, Bioresourc. Technol. 144 (2013) 67-73.

[27] P.M. Rao, A. Wolfson, M.V. Landau, M. Herskowitz, Catal. Commun. 5 (2004) 327-331.

[28] M.A. Hanif, S. Nisar, U. Rashid, Catal. Rev. 59 (2017) 165-188.

[29] K. Shimizu, H. Furukawa, N. Kobayashi, Y. Itaya, A. Satsuma, Green Chem. 11 (2009) 1627-1632.

[30] F. Guo, Z. Fang, T. Zhou, Bioresourc. Technol. 112 (2012) 313-318.

[31] F. Guo, Z. Xiu, Z. Liang, Appl. Energ. 98 (2012) 47-52.

[32] K. Shimizu, K. Niimi, A. Satsuma, Appl. Catal. A-Gen. 349 (2008) 1-5.

[33] Q.Y. Liu, W.L. Wu, J. Wang, X.Q. Ren, Y.R. Wang, Microp. Mesopor. Mat. 76 (2004) 51-60.

[34] J.A. Dias, E.C. Sílvia, C.L. Dias, Microporous Mesoporous Mat. 76 (2004) 221-232.

[35] S. Wu, J. Wang, W. Zhang, X. Ren, Catal. Lett. 125 (2008) 308–314.

[36] K. Narasimharao，D.R. Brown，A.F. Lee，A.D. Newman，P.F. Siril，S.J. Tavener，K. Wilson，J Catal. 248 (2007) 226-234

[37] N. Lingaiah, K. MohanReddy, N. SeshuBabu, K. NarasimhaRao, I. Suryanarayana, P.S. SaiPrasad, Catal. Commun. 7 (2006) 245-250.

[38] X. Guo, C.H. Zhu, F. Guo, Bioresources 11 (2016) 2457-2469.

[39] V. Choudhary, S.I. Sandler, D.G. Vlachos, ACS Catal. 2 (2012) 2022-2028.

[40] I. Agirrezabal-Telleria, I. Gandarias, P.L. Arias, Catal. Today 234 (2014) 42-58.

[41] A.S. Dias, S. Lima, M. Pillinger, A.A. Valente, Catal. Lett. 114 (2007) 151-160.

[42] A.S. Dias, M. Pillinger, A.A. Valente, J. Catal. 229 (2005) 414-423.

[43] L. Zhang, H. Yu, P. Wang, Y. Li, Bioresource Technol. 151(2014)355-360.

[44] X. Hu, R.J.M. Westerhof, D. Dong, L. Wu, C.Z. Li, ACS Sustainable Chem. Eng., 11 (2014) 2562–2575.

[45] K.J. Zeitsch, Chem. Innovat. 30 (2000) 29-33.

[46] O. Yemiş, G. Mazza, Bioresource Technol. 102 (2011) 7371-7378.

Tables caption

Table 1 Effect of surficial Sn^{4+} and Cs^{+} attribution on furfural yield and D-xylose conversion.

Table 2 BET surface area and pore properties of the heteropolyacid salts

Figures captions

Figure 1. SEM images of heteropolyacid salts: (a) $H_{2.5}Cs_{0.5}PW$, (b) $H_{0.5}Cs_{2.5}PW$, (c) $Sn_{0.5}CsPW$, (d) $Sn_{0.625}Cs_{0.5}PW$, (e) $Sn_{0.55}Rb_{0.8}PW$, (f) CH, (g) 30% $H_{0.5}Cs_{2.5}PW/CH$, (h) $Sn_{0.625}Cs_{0.5}PW/CH$.

Figure 2. XRD pattern for (a) $Sn_{0.625}Cs_{0.5}PW$; (b) $Sn_{0.5}CsPW$; (c) $Sn_{0.55}Rb_{0.8}PW$; (d) 16.7% $Sn_{0.625}Cs_{0.5}PW/CH$.

Figure 3. Nitrogen adsorption–desorption isotherm of $Sn_{0.625}Cs_{0.5}PW$.

Figure 4. Dehydration of D-xylose catalyzed by different solid heteropoly salts: a, H_2RbPW; b, $H_{0.5}Cs_{2.5}PW$; c, HKCsPW; d, HNH_4CsPW; e, $H_{0.5}Fe_{0.5}PW$; f, $HNi_{0.5}CsPW$; g, $Sn_{0.625}Cs_{0.5}PW$; h: $H_{0.5}Ce_{0.5}CsPW$; l, H_2SO_4; m, HCl; n, CH_3COOH. Conditions: D-xylose 0.1 g, amount of catalyst 0.08 g, H_2O 20 ml, 200 °C for 3 h.

Figure 5. Effect of initial concentration of D-xylose on dehydration: (a) in water (200 °C for 3.5 h); (b) in DMSO/H_2O mixture with 1:1 volume ratio (180 °C for 3 h).

Figure 6. Furfural selectivity (mol%) vs. solvent/H_2O mixtures with volume ratio of 1:1 (D-xylose 0.1 g, $Sn_{0.625}Cs_{0.5}PW$ 0.08 g, solvent 20 ml, 200 °C, 3h)

Figure 7. Effect of reaction temperature on dehydration in DMSO/H_2O mixture with 1:1 volume ratio (D-xylose 0.1 g, $Sn_{0.625}Cs_{0.5}PW$ 0.08 g, DMSO/H_2O 20 ml).

Figure 8. The effect of $Sn_{0.625}Cs_{0.5}PW$ loading amount on D-xylose conversion and furfural yield. (DMSO-H_2O with 1:1 volume ratioratio 20 ml, D-xylose 0.1 g, $Sn_{0.625}Cs_{0.5}PW$ 0.08 g, 200 °C, 3 h)

Fig. 9. Effect of recycling of 16.7 wt % $Sn_{0.625}Cs_{0.5}PW/CH$ on D-xylose conversion and furfural yield (D-xylose 0.1 g, $Sn_{0.625}Cs_{0.5}PW$ 0.08 g, DMSO/H_2O 20 ml, 200 °C, 3 h)

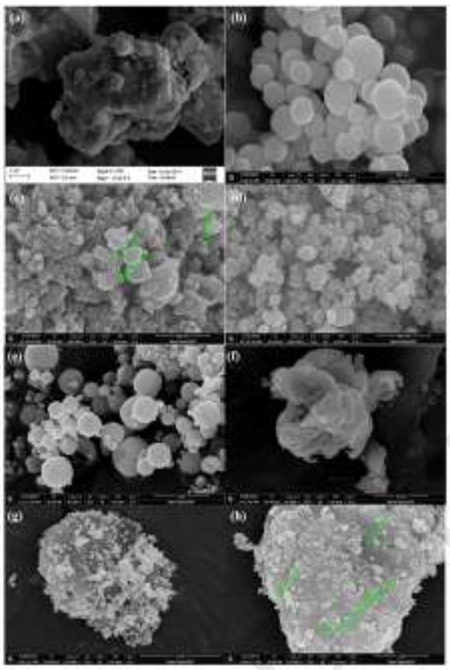

Figure 1. SEM images of heteropolyacid salts: (a) $H_{2.5}Cs_{0.5}PW$, (b) $H_{0.5}Cs_{2.5}PW$, (c) $Sn_{0.5}CsPW$, (d) $Sn_{0.625}Cs_{0.5}PW$, (e) $Sn_{0.55}Rb_{0.8}PW$, (f) CH, (g) 30% $H_{0.5}Cs_{2.5}PW/CH$, (h) $Sn_{0.625}Cs_{0.5}PW/CH$.

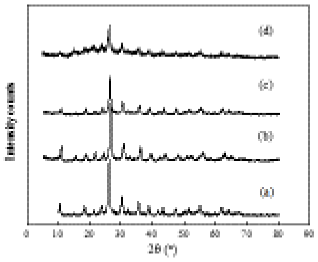

Figure 2. XRD pattern for (a) $Sn_{0.625}Cs_{0.5}PW$; (b) $Sn_{0.5}CsPW$; (c) $Sn_{0.55}Rb_{0.8}PW$; (d) 16.7 wt % $Sn_{0.625}Cs_{0.5}PW/CH$.

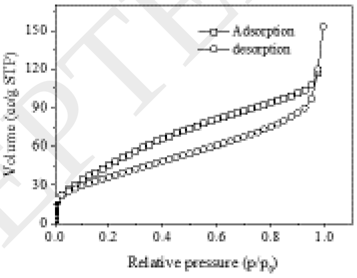

Figure 3. Nitrogen adsorption–desorption isotherm of $Sn_{0.625}Cs_{0.5}PW$.

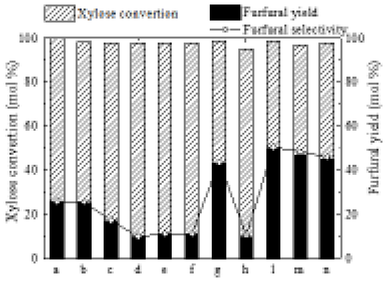

Figure 4. Dehydration of D-xylose catalyzed by different solid heteropoly salts: a, H_2RbPW; b, $H_{0.5}Cs_{2.5}PW$; c, HKCsPW; d, HNH_4CsPW; e, $H_{0.5}Fe_{0.5}PW$; f, $HNi_{0.5}CsPW$; g, $Sn_{0.625}Cs_{0.5}PW$; h: $H_{0.5}Ce_{0.5}CsPW$; l, H_2SO_4; m, HCl; n, CH_3COOH. Conditions: D-xylose 0.1 g, amount of catalyst 0.08 g, H_2O 20 ml, 200 °C for 3 h.

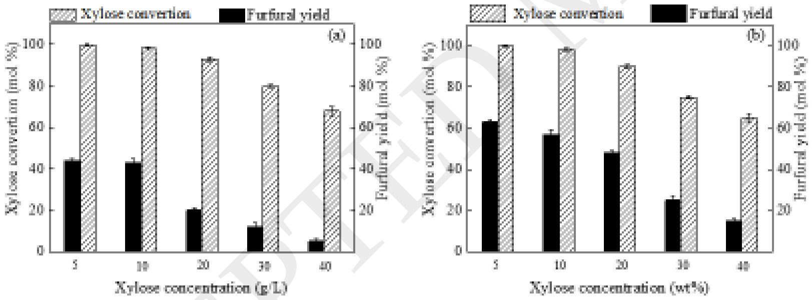

Figure 5. Effect of initial concentration of D-xylose on dehydration: (a) in water (200 °C for 3.5 h); (b) in DMSO/H_2O mixture with 1:1 volume ratio (180 °C for 3 h).

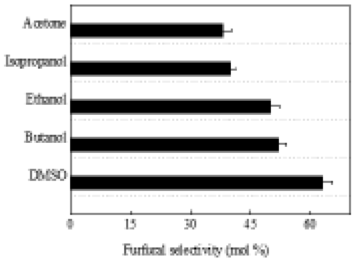

Figure 6. Furfural selectivity (mol%) vs. solvent/H_2O mixtures with volume ratio of 1:1 (D-xylose 0.1 g, $Sn_{0.625}Cs_{0.5}PW$ 0.08 g, solvent 20 ml, 200 ºC, 3h)

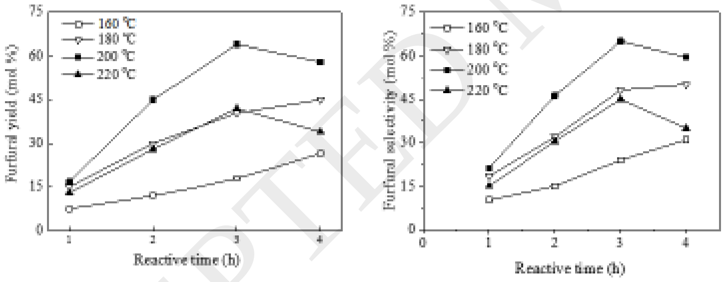

Figure 7. Effect of reaction temperature on dehydration in DMSO/H_2O mixture with 1:1 volume ratio (D-xylose 0.1 g, $Sn_{0.625}Cs_{0.5}PW$ 0.08 g, DMSO/H_2O 20 ml).

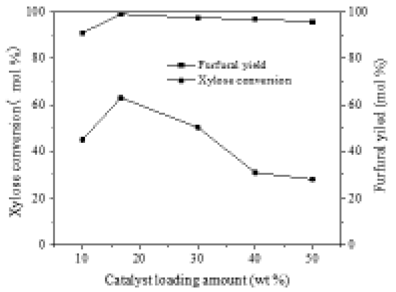

Figure 8. The effect of $Sn_{0.625}Cs_{0.5}PW$ loading amount on D-xylose conversion and furfural yield. (DMSO-H_2O with 1:1 volume ratio 20 ml, D-xylose 0.1 g, $Sn_{0.625}Cs_{0.5}PW$ 0.08 g, 200 °C, 3 h)

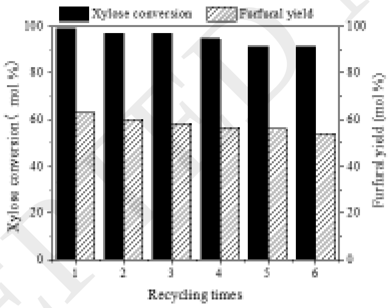

Fig. 9. Effect of recycling of 16.7 wt % $Sn_{0.625}Cs_{0.5}PW$/CH on D-xylose conversion and furfural yield (D-xylose 0.1 g, $Sn_{0.625}Cs_{0.5}PW$ 0.08 g, DMSO/H_2O 20 ml, 200°C, 3 h)

Table 1 Effect of surficial Sn^{4+} and Cs^+ attribution on furfural yield and D-xylose conversion

Molecular formula	Sn mol %	Cs mol %	Furfural yield (mol %)	D-xylose conversion (mol %)
$H_{1.5}Sn_{0.25}Cs_{0.5}PW_{12}O_{40}$	0.452	0.905	16.7	99
$Sn_{0.5}CsPW_{12}O_{40}$	0.917	1.147	25.3	99
$Sn_{0.55}Cs_{0.8}PW_{12}O_{40}$	1.012	1.472	33.5	99
$Sn_{0.625}Cs_{0.5}PW_{12}O_{40}$	1.155	0.924	44.4	99
$Sn_{0.625}Cs_{0.5}PW_{12}O_{40}$	1.155	0.924	39.6	99

Error of measurement = ±3%.

Reaction conditions: D-xylose 0.2 g, $Sn_{0.625}Cs_{0.5}PW$ 0.16 g, solvent 20 ml, 200 °C, 3.5 h, in water media.

Table 2 BET surface area and pore properties of the heteropolyacid salts

	Surface area (m^2/g)[a]	Pore diameter (nm)	Pore volume (cm^3/g)	Ref.
H_3PW	5	> 48.0[b]	-	[34]
Cs_3PW	156	19.4[b]	14.1	[34]
$Sn_{0.625}Cs_{0.5}PW$	140	11[c]	0.32	In this study
16.7 wt% $Sn_{0.625}Cs_{0.5}PW/CH$	219	9.6[c]	0.39	In this study

[a] BET equation.

[b] Estimated from XRD line width of peak ~26°.

[c] BJH equation.